# Nearest and next-nearest superexchange interactions in orthorhombic perovskite manganites $R\mathrm{MnO_3}$ ($R$=rare earth)

Beom Hyun Kim and B. I. Min
*Department of Physics, PCTP, Pohang University of Science and Technology, Pohang 790-784, Korea*
(Received 23 July 2009; published 24 August 2009)

To explore the spiral and $E$-type magnetic orders observed in orthorhombic perovskite manganites $R\mathrm{MnO_3}$ ($R$: rare-earth element), we have studied the magnetic superexchange interaction in $R\mathrm{MnO_3}$ based on the microscopic model incorporating the $\mathrm{GdFeO_3}$-type octahedral tilting and the Jahn-Teller (JT) distortion. We have found that (i) the account of $t_{2g}$ electrons is essential to describe both the nearest-neighbor (NN) and next-nearest-neighbor (NNN) superexchange interactions, (ii) the JT distortion angle as well as the octahedral tilting and the JT distortion strength is an important factor for the superexchange interactions, and (iii) two NNN interactions in the $ab$ plane are anisotropic but are both antiferromagnetic. We have determined the magnetic-phase diagram of $R\mathrm{MnO_3}$ and discussed the magnetic ground states in relation to the experiments.

DOI: 10.1103/PhysRevB.80.064416 PACS number(s): 75.10.−b, 75.30.Et, 71.70.−d

## I. INTRODUCTION

The magnetic structures of orthorhombic rare-earth manganites $R\mathrm{MnO_3}$ ($R$: rare-earths) are very complicated, especially for $R$ with small ionic radius ($r_R$). The early $R\mathrm{MnO_3}$'s with large $r_R$ have the stable orthorhombic ($Pbnm$) perovskite structure. However, for the late $R\mathrm{MnO_3}$'s ($R$=Ho-Lu) with small $r_R$, the orthorhombic phase is metastable in nature, and so it can be synthesized only under high pressure. The early $R\mathrm{MnO_3}$'s ($R$=La-Gd) exhibit a rather simple $A$-type antiferromagnetic (AF) structure, and the transition temperature $T_N$ decreases with decreasing $r_R$ from La to Gd. In contrast, $\mathrm{TbMnO_3}$ and $\mathrm{DyMnO_3}$ which are next to $\mathrm{GdMnO_3}$ undergo the complex magnetic transitions, first to an incommensurate sinusoidal order, and then, upon further cooling, to an incommensurate spiral order accompanied by the ferroelectric order.[1,2] On the other hand, $R\mathrm{MnO_3}$'s with smaller $r_R$ including $\mathrm{YMnO_3}$ were reported to have the $E$-type order, in which the spins in the $ab$-plane are arranged with "up-up-down-down" order and those along the $c$ axis are AF.[3]

The orthorhombic $R\mathrm{MnO_3}$'s suffer two different lattice distortions. The first is a cooperative octahedral tilting, driven by the mismatch of $R$-O ($d_R$) and Mn-O ($d_M$) bond lengths. This causes the oxides to have the $\mathrm{GdFeO_3}$-type distortion in which the $\mathrm{MnO_6}$ octahedra are tilted cooperatively [see Fig. 1(a)]. The tilting angle ($\omega$) and two Mn-O-Mn bond angles ($\phi_1, \phi_2$) of orthorhombic $R\mathrm{MnO_3}$ are characterized by the tolerance factor $f \equiv d_R/\sqrt{2}d_M$. Plotted in Fig. 2(a) are the estimated $\omega$, $\phi_1$, and $\phi_2$ of orthorhombic $R\mathrm{MnO_3}$ for given $f$ in the scheme of Ref. 4. With decreasing $r_R$ from La to Lu, $\omega$ increases and so $\phi_1$ and $\phi_2$ are reduced monotonically. The second is an octahedral bond-length change due to Jahn-Teller (JT) active $\mathrm{Mn^{3+}}$ ions. Local $\mathrm{MnO_6}$ octahedra are elongated and shortened alternatively in the $ab$ plane and thereby the doubly degenerate $e_g$ orbitals are split to manifest the $C$-type orbital ordering (OO) [see Figs. 1(b) and 1(c)]. Figure 2(b) shows experimental data of the JT distortion strength ($\rho$) and the JT distortion angle ($\theta$) for $R\mathrm{MnO_3}$. With decreasing $r_R$, $\rho$ and $\theta$ increase first and then decrease possessing maxima near Gd. These structural modifications are thought to bring about the complex magnetic-phase diagram in orthorhombic $R\mathrm{MnO_3}$.[5–9]

The anisotropic hopping nature of the $C$-type OO induces the $A$-type AF order in the perovskite systems. Indeed the magnetic structure of $\mathrm{LaMnO_3}$ can be understood in terms of this picture.[10–13] The observed rapid drop of $T_N$ with decreasing $r_R$ is explained simply by the reduced hopping strength ($t \sim t_0 \cos\phi$) due to the increased octahedral tilting. According to the experiments, however, the AF interaction parameter along the $c$ axis, $J_c$, is more or less constant, even though the in-plane ferromagnetic (FM) interaction parameter, $J_{ab}$, decreases markedly.[14] Thus the above simple analysis is not adequate to explain such intriguing magnetic behavior in early $R\mathrm{MnO_3}$. Furthermore, there is controversy over the role of $t_{2g}$ electrons in stabilizing the $A$-type AF order even in $\mathrm{LaMnO_3}$. Ishihara *et al.*[11] claimed that the AF superexchange from $t_{2g}$ is essential while other theoretical groups[12,15] claimed that the $e_g$ only superexchange is the main mechanism.

It is no doubt that the JT distortion alters the magnetic interaction in $R\mathrm{MnO_3}$. As shown in Fig. 2(b), the JT parameters, $\rho$ and $\theta$, vary depending on $r_R$: $\theta$ is in between 107.6° and 117.8°, and $\rho_R/\rho_{\mathrm{La}}$ is in between 1.0 and 1.2. Concern-

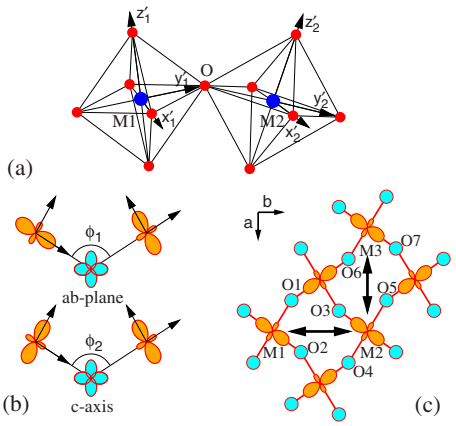


FIG. 1. (Color online) (a) Neighboring $\mathrm{MnO_6}$ octahedra in the orthorhombic perovskite $R\mathrm{MnO_3}$. (b) The OO patterns for two different Mn-O-Mn chains. (c) The NNN interaction channels.

 

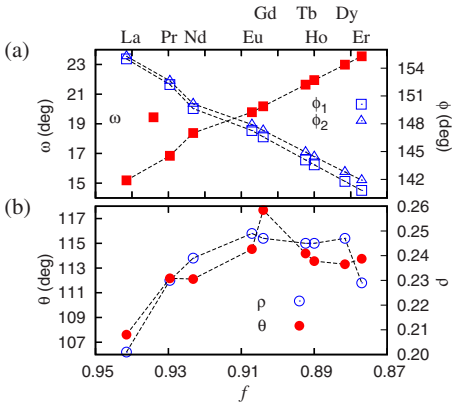


FIG. 2. (Color online) (a) Estimated octahedral tilting angle ($\omega$) and two Mn-O-Mn bond angles ($\phi_1$: in plane, $\phi_2$: $c$ axis) vs the tolerance factor $f$ for $R\mathrm{MnO_3}$. (b) Experimental data (Refs. 5–7) of the JT distortion strength ($\rho$) and distortion angle ($\theta$) vs $f$, where $\rho=\sqrt{q_2^2+q_3^2}$ and $\theta=\tan^{-1}(\frac{q_2}{q_3})$ with $q_2$ and $q_3$ being orthorhombic and tetragonal JT modes in the $O_h$ symmetry, respectively.

ing the effect of JT parameter $\theta$, two contrasting predictions were reported: Zhou and Goodenough[7] claimed that $J_{ab}$ is insensitive to $\theta$ but other experimental (Kim *et al.*[16]) and theoretical (Gontchar *et al.*[17] and Oleś *et al.*[18]) groups claimed the opposite.

When the octahedral tilting becomes strong, the Mn-O-Mn bond is significantly bent and two facing oxygens become close to each other as shown in Fig. 1(c). Then the hopping strength between the nearest-neighbor (NN) Mn ions is reduced and electrons are able to hop among next-nearest-neighbor (NNN) Mn sites through Mn-O-O-Mn paths. In this case, the NNN interactions as well as the NN interaction will play a role in stabilizing the magnetic structure. In fact, the NNN magnetic interactions were invoked to interpret the spiral and $E$-type magnetic structures for $R\mathrm{MnO_3}$ with small $r_R$.[3,8,19] However, there is no agreement even on the signs of the NNN magnetic interactions, $J_a$ and $J_b$, along the $a$ and $b$ axes. Kimura *et al.*[8] proposed that $J_a<0$ and $J_b>0$ for $\mathrm{HoMnO_3}$. On the contrary, neutron experiment by Kajimoto *et al.*[14] and band calculation by Xiang *et al.*[20] suggested both positive $J_a$ and $J_b$ for $\mathrm{TbMnO_3}$.

To resolve the above controversial issues on the magnetic structures of orthorhombic $R\mathrm{MnO_3}$, we have investigated systematically the NN and NNN superexchange interactions in $R\mathrm{MnO_3}$ with respect to the octahedral tilting and the JT distortion. We have determined the ground-state magnetic structures for $R\mathrm{MnO_3}$ based on the NN and NNN superexchange parameters obtained from the microscopic model for $R\mathrm{MnO_3}$.

## II. MICROSCOPIC MODEL

We have considered the following microscopic Hamiltonian for two linked $MO_6$ octahedra in Fig. 1(a):

TABLE I. Physical parameters in unit of [eV] for the orthorhombic $R\mathrm{MnO_3}$. $\Delta$ and $10D_q$ are the charge-transfer energy and the energy difference between $t_{2g}$ and $e_g$. The JT splitting energy ($\Delta_{JT}$) is given by $\Delta_{JT}=1.0\ \rho/\rho_{\mathrm{La}}$. The values of $t_{pd\sigma}$ and $t_{pp\sigma}$ refer to hopping strengths for fixed Mn-O and O-O distances by 2.0 Å. We set $t_{pd\pi}=-0.46t_{pd\sigma}$, $t_{pp\pi}=-0.25t_{pp\sigma}$, and assumed $t_{pd\sigma}\propto d^{-3.5}$, and $t_{pp\sigma}\propto d^{-2}$ (Ref. 22).

| $\Delta$ | $10Dq$ | $\Delta_{JT}$(La) | $U_d$ | $J_d$ | $U_p$ | $J_p$ | $\epsilon_p$ | $t_{pd\sigma}$ | $t_{pp\sigma}$ |
|---|---|---|---|---|---|---|---|---|---|
| 3.5 | 1.8 | 1.0 | 6.0 | 0.6 | 2.0 | 0.0 | 0.0 | −1.6 | 3.0 |

$$H=\sum_{i,\mu_i}\epsilon_{\mu_i}n_{\mu_i}+U_d\sum_{i,\mu_i\nu_i}n_{\mu_i}n_{\nu_i}-J_d\sum_{i,\mu_i\nu_i\sigma}n_{\mu_i\sigma}n_{\nu_i\sigma}+\sum_{l}\epsilon_p n_l+U_p\sum_{lm}n_l n_m-J_p\sum_{lm\sigma}n_{l\sigma}n_{m\sigma}+\sum_{\langle i,j\rangle\mu_i l\sigma}t^{\mu_i l}[d^{\dagger}_{\mu_i\sigma}c_{l\sigma}+\mathrm{H.c.}], \quad (1)$$

where $d^{\dagger}_{\mu_i\sigma}$ and $c_{l\sigma}$ are the creation operator of Mn $d$ electron with $\mu_i$ orbital and $\sigma$ spin states at $i$ site and the annihilation operator of O $p$ electron with $l$ orbital and $\sigma$ spin states, respectively. $U_L$ and $J_L$ ($L=d,p$) are on-site Coulomb and exchange interactions, respectively. The hopping parameters $t^{\mu_i l}$ are evaluated as functions of the two $p$-$d$ hopping parameters, $t_{pd\sigma}$ and $t_{pd\pi}$, according to Slater-Koster.[21] Because of strong cubic crystal field and JT distortion effects, $d$-orbital states are well described by the basis $\{|x_i'y_i'\rangle,|y_i'z_i'\rangle,|z_i'x_i'\rangle,|\theta_i\rangle,|\theta_i+\pi\rangle\}$ in the local $\{x_i',y_i',z_i'\}$ coordinate, where $|\theta\rangle$ is defined by $|\theta\rangle=\cos\frac{\theta}{2}|3z'^2-r^2\rangle+\sin\frac{\theta}{2}|x'^2-y'^2\rangle$. To consider the $C$-type distortion, $|\theta\rangle/|2\pi-\theta\rangle$-type OO in the $ab$ plane and $|\theta\rangle/|\theta\rangle$-type OO along the $c$ axis are assumed. The NN superexchange parameters $J_{ab}$ and $J_c$ are calculated in the perturbation framework for $U\gg t$, assuming that the magnetic interaction follows the Heisenberg type, $E=2J\vec{S}_1\cdot\vec{S}_2$, and the energy difference between $E_{\uparrow\uparrow}$ and $E_{\uparrow\downarrow}$ is given by $4JS^2$. The relevant physical parameters we have used are presented in Table I.

## III. MAGNETIC INTERACTION

In Fig. 3(a), results of $J_{ab}$ and $J_c$ are provided with varying the tilting angle $\omega$. For $\omega<23°$, $J_{ab}$ is negative while $J_c$ is positive, which refers to the typical $A$-type AF order for $R\mathrm{MnO_3}$ with large $r_R$. For $\omega>23°$, the magnetic structure is changed from $A$ through $G$ to $C$ type in our calculation. To examine the role of $t_{2g}$ electron hopping in the magnetic interaction, we have also performed calculations with setting $t_{pd\pi}=0.0$. Because $t_{2g}$ orbitals bond only with $p$ orbitals through the $\pi$ bonding, the treatment of $t_{pd\pi}=0.0$ helps us to inspect the $e_g$ electron only contribution to the superexchange interaction. Figure 3(a) reveals that both $J_{ab}$ and $J_c$ become negative for $t_{pd\pi}=0.0$, that is, the FM order will be stabilized in the $e_g$ only system. This result indicates that the inclusion of the $t_{2g}$ hopping is essential to stabilize the $A$-type AF order in $R\mathrm{MnO_3}$, supporting the scenario of Ishihara *et al.*[11]

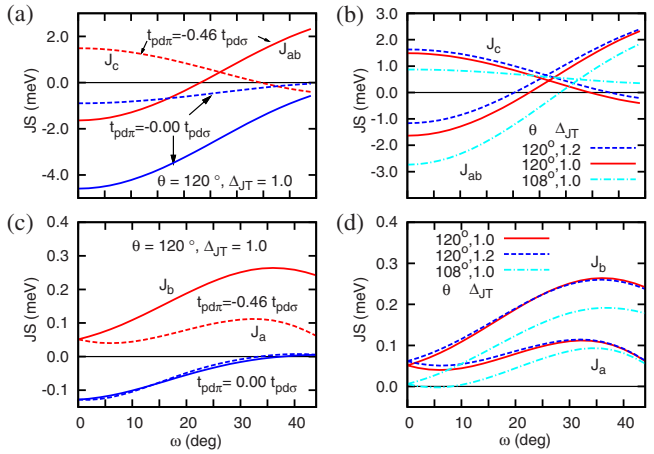


FIG. 3. (Color online) [(a) and (b)] The NN superexchange parameters $J_{ab}$ and $J_c$ as functions of the tilting angle ($\omega$) and the JT distortion ($\theta$,$\Delta_{JT}$). [(c) and (d)] The NNN superexchange parameters $J_a$ and $J_b$ as functions of $\omega$, $\theta$, and $\Delta_{JT}$.

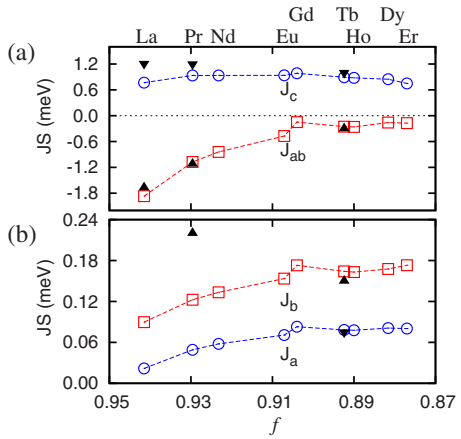


FIG. 4. (Color online) Theoretical (⊙ and ⊡) and experimental (▲ and ▼) results for (a) the NN and (b) the NNN superexchange parameters for $R$MnO$_3$. For PrMnO$_3$, only one NNN superexchange parameter $J_b$ was used in Ref. 14 for the experimental analysis and so the experimental value of $J_b$ in (b) gives rise to a measure of the maximum $J_b$.

Figure 3(b) shows the effects of JT parameters on $J_{ab}$ and $J_c$. For $\omega < 23°$, both $J_{ab}$ and $J_c$ are shifted down with decreasing $\theta$. $J_{ab}$ is changed a lot with $\theta$. This feature indicates that $J_{ab}$ is underestimated in usual theoretical works assuming $\theta$=120° because $107° \lesssim \theta \lesssim 118°$ for real $R$MnO$_3$. This result is consistent with existing experimental[16] and theoretical[17,18] results but is quite opposed to that of Zhou and Goodenough[7] who claimed that $J_{ab}$ is insensitive to $\theta$. On the other hand, the increase in the JT splitting energy $\Delta_{JT}$ shifts up both $J_{ab}$ and $J_c$ values: $J_{ab}$ becomes less negative while $J_c$ becomes more positive. This behavior of $J_{ab}$ with respect to $\Delta_{JT}$ is consistent with that by Zhou and Goodenough[7] in contrast to that with respect to $\theta$.

Figure 3(c) provides results for the NNN superexchange parameters $J_a$ and $J_b$. As shown in Fig. 1(c), $J_b$ ($J_a$) between $M1$ and $M2$ ($M2$ and $M3$) is mediated by four oxygens O1, O2, O3, and O4 (O3, O5, O6, and O7). To take care of the NNN interaction through Mn-O-O-Mn hopping, we have considered the additional O $p$-$p$ hopping $t^{p_i,p_j}$ between $p_i$ and $p_j$ orbitals (see Table I). Differently from the NN interaction, the NNN interaction in Fig. 3(c) shows anisotropic behavior depending on the direction: $J_b$ is always larger than $J_a$. Note that, for GdFeO$_3$-type distortion, the rotational axis of octahedra is close to the $b$ axis in the $Pbnm$ symmetry.[23] Hence the hopping anisotropy results from distinctly bent hopping channels and gives rise to the anisotropic NNN interaction. It is tempting to expect that $e_g$ electrons produce the AF NNN interaction because two NNN Mn ions have the same orbital patterns. Inspecting oxygen positions closely, however, the OO provides different patterns depending on the interaction channels. For $M1$-O2-O3-$M2$ channel, both $M1$-O2 and O3-$M2$ bonds are elongated, while, for $M1$-O2-O4-$M2$ channel, one bond ($M1$-O2) is elongated but the other (O4-$M2$) is shortened. For a hopping electron, the former appears to be ferro-OO, whereas the latter to be antiferro-OO. The latter is dominant for small $\omega$, but with increasing $\omega$, the former becomes larger and larger, and so, when $t_{pd\pi}$=0.0, the NNN interaction changes from FM to AF for $\omega > 30°$. Therefore, as shown in Fig. 3(c), the $t_{2g}$ hopping which always stabilizes the AF interaction plays an important role in determining the sign of the NNN interaction.

Figure 3(d) demonstrates that the JT distortion also affects the NNN interaction: the positive interaction diminishes in magnitude as $\theta$ descends from 120°. Its behavior resembles that of the NN interaction. The effect of the distortion strength, however, is weaker than in $J_{ab}$. It is because the $t_{2g}$ orbitals, which contribute to the NNN interaction predominantly, is less active in the JT distortion than $e_g$.

Figure 4 provides the NN and NNN superexchange parameters for $R$MnO$_3$, which are obtained using the octahedral structural parameters shown in Fig. 2. In Fig. 4(a), the rapid drop of the FM $J_{ab}$ with decreasing $r_R$ and the weak $r_R$ dependence of the AF $J_c$ are achieved in agreement with the experiments. For $R$=La-Gd, the increase in $\omega$ and $\theta$ contribute cooperatively to suppress $J_{ab}$. In contrast, for $J_c$, one effect compensates for another making $J_c$ nearly constant. Indeed our theoretical values of $J_{ab}$ and $J_c$ are in good agreement with experimental data for LaMnO$_3$, PrMnO$_3$, and TbMnO$_3$ which were obtained from the inelastic neutron scattering.[14,24]

As for the NNN interaction in Fig. 4(b), both $J_a$ and $J_b$ are positive and increase gently as $R$ goes from La to Gd. For smaller $r_R$, they are nearly constant due to opposite contributions of $\omega$ and $\theta$, as in $J_{ab}$ and $J_c$. For $J_a$ and $J_b$, experimental data[14] exist only for TbMnO$_3$. They are again in good agreement with our results: both are positive and $J_b$ is about twice larger than $J_a$. Similar values of $J_a$ and $J_b$ were reported for TbMnO$_3$ from the band-structure study too.[20]

## IV. MAGNETIC PHASE DIAGRAM

Using the theoretical superexchange parameters in Fig. 4, we have examined the magnetic ground states of $R$MnO$_3$. We have considered both the Ising and Heisenberg spin systems with cubic lattices ($16 \times 16 \times 4$), which are solved by employing the Monte Carlo method based on the Wolff's

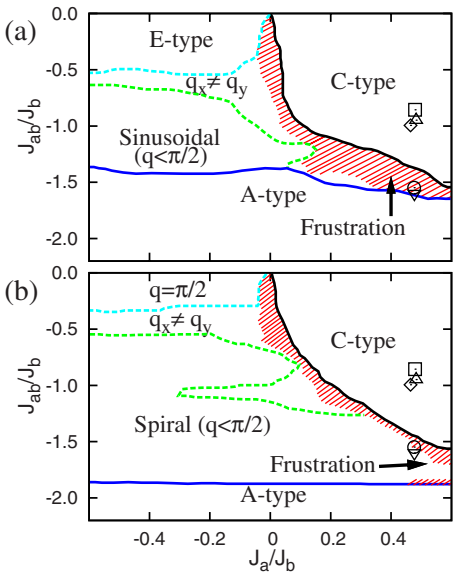


FIG. 5. (Color online) Magnetic-phase diagrams for (a) the Ising spin system at $T=0.4J_c/k_B$ and (b) the classical Heisenberg spin system at $T=0.1J_c/k_B$. $J_b$ and $J_c$ are set to be positive with $J_c/J_b=2.0$. In the frustration region of hatched lines, $S_{\mathbf{q}}$ has two or more peaks or broad distribution, instead of single maximum peak. The corresponding exchange parameters for $R\mathrm{MnO_3}$'s with small $r_R$ obtained in Fig. 4 are represented by square (Gd), circle (Tb), triangle (Dy), inverse triangle (Ho), and rhombus (Er), respectively. For $R$=La-Eu, the corresponding exchange parameters are located in the $A$-type region.

algorithm.[25] Figure 5 shows the resulting magnetic phase diagram with respect to $J_{ab}$ and $J_a$. Here, we considered the behavior of the magnetic order parameter, $\vec{S}_{\mathbf{q}}=\frac{1}{N}\Sigma_i \vec{S}_i e^{i\mathbf{q}\cdot\vec{r}_i}$, to determine the stable magnetic phase. The $A$-type ground state is obtained for $R$=La-Eu, for which $J_{ab}/J_b<-2.0$ and $J_a/J_b\sim 0.4$, as is consistent with the experiment. But for small $r_R$ cases with $J_a/J_b>0$, there appears discrepancy between theoretical and experimental ground states. For the Ising-type spin system in Fig. 5(a), the magnetic ground state for $J_a/J_b>0$ corresponds to the $C$-type or the frustrated structure rather than the $E$-type or the spiral order. The spiral, sinusoidal, and $E$-type orders are realized only for $J_a/J_b<0$. Of course, the spiral order is possible for the Heisenberg-type spin system [Fig. 5(b)], even though the stable region for $J_a/J_b>0$ is much smaller than that for $J_a/J_b<0$. Nevertheless, it seems to be unlikely for the $E$-type order to appear within the classical spin systems, unless $J_a$ and $J_b$ have opposite signs.

Kimura *et al.*[8] argued that, depending on the ratio of $J_{ab}/J_b$, the in-plane magnetic state changes from FM through sinusoidal AF to the spiral or the $E$-type order for $J_a<0$ and $J_b>0$. But, as mentioned earlier, existing experimental[14] and band-calculational[20] results as well as ours indicate that both $J_a$ and $J_b$ are positive so that their proposition is not plausible. On the other hand, Zhou and Goodenough[7] proposed without invoking the NNN interactions that the segregation of $J_{ab}>0$ and $J_{ab}<0$ bonds would bring the $E$ phase. But there is no direct evidence to verify their scenario. There were also studies to stabilize the $E$-phase incorporating the double-exchange interaction.[19,26] This approach, however, is not so convincing, considering insulating nature of $R\mathrm{MnO_3}$ with large on-site Coulomb interaction among the half-filled $e_g$ orbitals. Therefore more studies are required to clarify the magnetic ground state of orthorhombic perovskite $R\mathrm{MnO_3}$ with small $r_R$.

## V. CONCLUSION

We have studied the NN and NNN superexchange interactions in orthorhombic $R\mathrm{MnO_3}$ with respect to the orthorhombic structural parameters. Not only the octahedral tilting and the JT distortion strength but also the $t_{2g}$ hopping and the JT distortion angle are found to be essential to describe the NN and NNN superexchange interactions. Our results for the NN and NNN exchange parameters are in good agreement with the experimental data, but, with the NNN exchange parameters $J_a/J_b>0$, there exists difficulty in explaining the $E$-type order observed for $R\mathrm{MnO_3}$ with small $r_R$.

## ACKNOWLEDGMENTS

This work was supported by the NRF (Grant No. 2009-0079947) and by the POSTECH Research Fund.

[1] T. Kimura, T. Goto, H. Shintani, K. Ishizaka, T. Arima, and Y. Tokura, Nature (London) **426**, 55 (2003).
[2] M. Kenzelmann, A. B. Harris, S. Jonas, C. Broholm, J. Schefer, S. B. Kim, C. L. Zhang, S.-W. Cheong, O. P. Vajk, and J. W. Lynn, Phys. Rev. Lett. **95**, 087206 (2005).
[3] A. Muñoz, M. T. Casáis, J. A. Alonso, M. J. Martínez-Lope, J. L. Martínez, and M. T. Fernández-Díaz, Inorg. Chem. **40**, 1020 (2001).
[4] M. O'Keeffe and B. G. Hyde, Acta Crystallogr., Sect. B: Struct. Crystallogr. Cryst. Chem. **33**, 3802 (1977); M. W. Lufaso and P. M. Woodward, Acta Crystallogr., Sect. B: Struct. Crystallogr. Cryst. Chem. **57**, 725 (2001).
[5] J. A. Alonso, M. J. Martínez-Lope, M. T. Casais, and M. T. Fernández-Díaz, Inorg. Chem. **39**, 917 (2000).
[6] B. Dabrowski, S. Kolesnik, A. Baszczuk, O. Chmaissem, T. Maxwell, and J. Mais, J. Solid State Chem. **178**, 629 (2005).
[7] J.-S. Zhou and J. B. Goodenough, Phys. Rev. Lett. **96**, 247202 (2006).
[8] T. Kimura, S. Ishihara, H. Shintani, T. Arima, K. T. Takahashi, K. Ishizaka, and Y. Tokura, Phys. Rev. B **68**, 060403(R) (2003).
[9] M. Tachibana, T. Shimoyama, H. Kawaji, T. Atake, and E. Takayama-Muromachi, Phys. Rev. B **75**, 144425 (2007).
[10] T. Mizokawa and A. Fujimori, Phys. Rev. B **51**, 12880 (1995); **54**, 5368 (1996).
[11] S. Ishihara, J. Inoue, and S. Maekawa, Phys. Rev. B **55**, 8280 (1997).

[12] L. F. Feiner and A. M. Oleś, Phys. Rev. B **59**, 3295 (1999).
[13] H. Meskine, H. König, and S. Satpathy, Phys. Rev. B **64**, 094433 (2001).
[14] R. Kajimoto, H. Mochizuki, H. Yoshizawa, H. Shintani, T. Kimura, and Y. Tokura, J. Phys. Soc. Jpn. **74**, 2430 (2005).
[15] M. Kataoka, J. Phys. Soc. Jpn. **73**, 1326 (2004).
[16] M. W. Kim, S. J. Moon, J. H. Jung, J. Yu, S. Parashar, P. Murugavel, J. H. Lee, and T. W. Noh, Phys. Rev. Lett. **96**, 247205 (2006).
[17] L. E. Gontchar, A. E. Nikiforov, and S. E. Popov, J. Magn. Magn. Mater. **223**, 175 (2001).
[18] A. M. Oleś, L. F. Feiner, P. Horsch, and G. Khaliullin, Phys. Status Solidi B **243**, 89 (2006).
[19] S. Dong, R. Yu, S. Yunoki, J.-M. Liu, and E. Dagotto, Phys. Rev. B **78**, 155121 (2008).
[20] H. J. Xiang, S.-H. Wei, M.-H. Whangbo, and J. L. F. Da Silva, Phys. Rev. Lett. **101**, 037209 (2008).
[21] J. C. Slater and G. F. Koster, Phys. Rev. **94**, 1498 (1954).
[22] W. A. Harrison, *Electronic Structure and the Properties of Solids* (Dover, New York, 1989).
[23] J.-S. Zhou and J. B. Goodenough, Phys. Rev. Lett. **94**, 065501 (2005).
[24] K. Hirota, N. Kaneko, A. Nishizawa, and Y. Eondoh, J. Phys. Soc. Jpn. **65**, 3736 (1996).
[25] U. Wolff, Phys. Rev. Lett. **62**, 361 (1989).
[26] T. Hotta, M. Moraghebi, A. Feiguin, A. Moreo, S. Yunoki, and E. Dagotto, Phys. Rev. Lett. **90**, 247203 (2003).